

ACCEPTED MANUSCRIPT

Functional screen printed RFID tags on flexible substrates, facilitating low-cost and integrated point-of-care diagnostics

To cite this article before publication: Suzanne Smith *et al* 2018 *Flex. Print. Electron.* in press <https://doi.org/10.1088/2058-8585/aabc8c>

Manuscript version: Accepted Manuscript

Accepted Manuscript is “the version of the article accepted for publication including all changes made as a result of the peer review process, and which may also include the addition to the article by IOP Publishing of a header, an article ID, a cover sheet and/or an ‘Accepted Manuscript’ watermark, but excluding any other editing, typesetting or other changes made by IOP Publishing and/or its licensors”

This Accepted Manuscript is © 2018 IOP Publishing Ltd.

During the embargo period (the 12 month period from the publication of the Version of Record of this article), the Accepted Manuscript is fully protected by copyright and cannot be reused or reposted elsewhere.

As the Version of Record of this article is going to be / has been published on a subscription basis, this Accepted Manuscript is available for reuse under a CC BY-NC-ND 3.0 licence after the 12 month embargo period.

After the embargo period, everyone is permitted to use copy and redistribute this article for non-commercial purposes only, provided that they adhere to all the terms of the licence <https://creativecommons.org/licenses/by-nc-nd/3.0>

Although reasonable endeavours have been taken to obtain all necessary permissions from third parties to include their copyrighted content within this article, their full citation and copyright line may not be present in this Accepted Manuscript version. Before using any content from this article, please refer to the Version of Record on IOPscience once published for full citation and copyright details, as permissions will likely be required. All third party content is fully copyright protected, unless specifically stated otherwise in the figure caption in the Version of Record.

View the [article online](#) for updates and enhancements.

Functional screen printed RFID tags on flexible substrates, facilitating low-cost and integrated point-of-care diagnostics

Suzanne Smith^{1,2}, Adelaide Oberholzer¹, Kevin Land¹, Jan G. Korvink² and Dario Mager²

¹ Council for Scientific and Industrial Research (CSIR), Meiring Naude Road, Brummeria, Pretoria, South Africa, 0001

² Karlsruhe Institute of Technology (KIT), Karlsruhe, Germany

Keywords

screen printing, flexible substrates, low-cost substrates, printed UHF RFID tags, printed electronics, paper-based diagnostics

Abstract

This work explores the practical functionality of ultra-high frequency (UHF) radio frequency identification (RFID) tags screen printed onto various low-cost, flexible substrates. The need for integrated and automated low-cost point-of-care diagnostic solutions has driven the development of automated sensing and connectivity for implementation with these devices. This work explores wireless communication for paper-based point-of-care diagnostic solutions through screen printing of UHF RFID tags onto various low-cost and flexible substrates. Manual screen printing and assembly of RFID sensor integrated circuit packages and UHF RFID dipole antennas onto various substrates was performed and the practical functionality of these tags was assessed. Print quality including parameters such as resistance, roughness and print thickness are reported to illustrate the effect of the substrate on the printed result. Practical read range measurements are presented for the various tags in passive and active modes, as well as with a load connected, for different tag orientations. Results showed that the tags are adequate for clinical requirements with read ranges of at least 75 mm achieved in passive mode across the different substrates. Our results indicate that a variety of low-cost substrates can be utilized as different packaging and label options for paper-based diagnostic tests. This work presents the feasibility of implementing such devices towards low-cost, integrated point-of-care diagnostics, using straightforward fabrication techniques and realistic testing environments to illustrate the possibilities.

1. Introduction

The goal of this work is ultimately to develop low-cost, all-printed sensing, read-out and connectivity components for point-of-care diagnostic applications. A major component towards achieving this goal is to investigate different types of substrates onto which these connected sensors can be printed. This work explores the practical functionality of ultra-high frequency (UHF) radio frequency identification (RFID) tags with sensing capabilities printed onto various flexible substrates that could be applied as different packaging and label options directly onto paper-based diagnostic tests and/or integrated as part of the paper-based diagnostic device itself.

The need for effective point-of-care diagnostics, particularly in resource-limited settings, has been emphasised by the World Health Organisation, who have established the ASSURED principles (Affordable, Sensitive, Specific, User-Friendly, Rapid and Robust, Equipment-free and Deliverable to end users) [1]. In addition there has been a drive towards implementing connectivity of devices, as current methods in resource-constrained or rural clinics use manual data capturing. This introduces immense challenges in the tracking of samples and results between the clinic and laboratory [2], as well as storing and back-up of results and data [3], and can cause delays and errors in recording of patient results. Automated digital data capture would be optimal to enable result storage, as well as the ability to access, share and file results. A number of equipment manufacturers have started to implement connectivity solutions for their instruments. As an example GeneXpert utilizes connectivity software platforms such as C360 by Cepheid or software by third-party companies and organizations including the Connected Diagnostics Platform by FIND. However, modems and internet connectivity are required and can be problematic in resource-limited settings.

Paper-based microfluidics have led to the evolution of low-cost point-of-care diagnostics suitable to resource-constrained settings that meet many of the ASSURED principles [4,5]. In addition, printed electronics enable sensors, processing and readout to be implemented on paper and flexible substrates [6]. Integration of paper-based diagnostics with printed functional components is currently being explored [7,8], with a clear need for automated and connected solutions to be realized through digital capturing and communication of the test result obtained from the paper-based diagnostic device. Towards achieving this goal, we examine a number of different paper-based and flexible substrates and assess the printability and functionality of a wireless communication module in the form of a RFID sensing tag onto these substrates.

Printing of antennas onto different substrates has been explored for specialized printed electronics substrates [9] and cardboard or recycled substrates using both inkjet [10] and screen printing techniques [11,12]. UHF RFID antenna designs typically have simple form factors, which are easier to print, and have longer read ranges than near field communication (NFC) implementations, where near-contact methods are utilized from a reader device such as a mobile phone. UHF RFID enables a “black box” reader solution to be implemented, a favourable implementation for rural clinics [13], eliminating the risk of theft or tampering with the reader device, while the disposable RFID tag can be either passive (without a battery) or active (with a battery), the former reducing the cost considerably and increasing the long term reliability.

We investigate a printed UHF RFID tag design, utilizing a sensing RFID integrated circuit (IC) (SL900A-DK-STQFN16, ams, Austria), to provide a compact, integrated solution that could enable automated read-out and communication of results to an external device in a wireless, contamination-free manner. These tags also enable identification, verification and tracking of the devices and allow for data to be logged in real time towards fully integrated and connected point-of-care diagnostic

1
2
3 solutions. The SL900A is advantageous for both detection and connectivity of paper-based
4 diagnostics as it is a single chip solution with extensive sensing capabilities, where resistance,
5 capacitance, voltage and current can be measured. The IC complies with the Electronic Product Code
6 (EPC Gen2 1.2), operating in the UHF band, with read distance in the cm to m range for a wireless
7 solution to be realized using a straightforward dipole antenna design that can easily be printed.
8
9

10 The sensing capabilities of this IC have previously been shown for fluidic detection on photo paper
11 [14], but printing of the tag antenna has been limited to printed electronics substrates such as
12 polyimide [15,16], with one example of printing onto cardboard packaging [17]. We expand on
13 existing investigations of SL900A-based RFID tags by exploring the feasibility of printing and
14 assembly of these tags onto a variety of substrates that could be applicable in the development of low-
15 cost point-of-care diagnostic devices for health and environmental applications. The goal is to
16 integrate a low-cost yet reliable analysis and communication unit with paper-based microfluidics,
17 thereby transforming a straightforward paper test strip into an automated, complete diagnostic device.
18
19

20 This work aims to assess the feasibility of using various substrates ranging in functionality,
21 characteristics and cost, for implementing manually screen printed and assembled RFID sensing tags.
22 The substrates include specialized papers optimized for either paper-based diagnostics or printed
23 electronics, low-cost, standard printing and packaging papers, and adhesive vinyl substrates. Print
24 quality of tag antennas was assessed across various substrates. Practical functionality of the tags was
25 investigated by performing read range tests to assess the read ranges for detecting the tags as well
26 reading out sensor values. Tags were tested in both passive and active modes, as well as with a load
27 attached in real-world settings to assess practical functionality of the tags, potentially in a rural clinic
28 environment. Varying orientations of the printed tags to the reader were also tested to assess the less
29 than optimal/non-ideal test situations that may result in a real-world testing environments.
30
31
32
33

34 2. Methods

35 Characterization of screen printed RFID tags on 20 different substrates (Table 1) was performed. Tag
36 antennas and additional electronic circuitry required for the RFID sensing chip to be integrated as part
37 of the device were printed onto each substrate. Manual screen printing was performed using a
38 modified stencil printer (ZelPrint LT300, LPKF Laser and Electronics, Germany). Printing quality
39 was characterized using electrical resistance measurements and brightfield microscopy techniques.
40 Practical functionality of the tag antennas was assessed by performing read range tests. The screen
41 printed RFID tags were compared to printed circuit board (PCB) devices of the tag antenna (category
42 CB, Table 1), as a benchmark, including the development kit (SL900A-DK-STQFN16, AMS,
43 Austria) and a milled PCB of the tag antenna manufactured and assembled in-house.
44
45
46
47
48
49
50
51
52
53
54
55
56
57
58
59
60

2.1. RFID tag design

The tag design was based on the reference design implemented as part of the development kit and consists of a dipole antenna resonating at 868 MHz. A 39 nH surface mount device (SMD) inductor is connected to one arm of the antenna to match the input impedance. Dipole antennas have advantageous omni-directional characteristics, allowing for flexibility in the positioning of the tag relative to the reader. Figure 1 shows the tag design used for printing, along with the points used for resistance measurements.

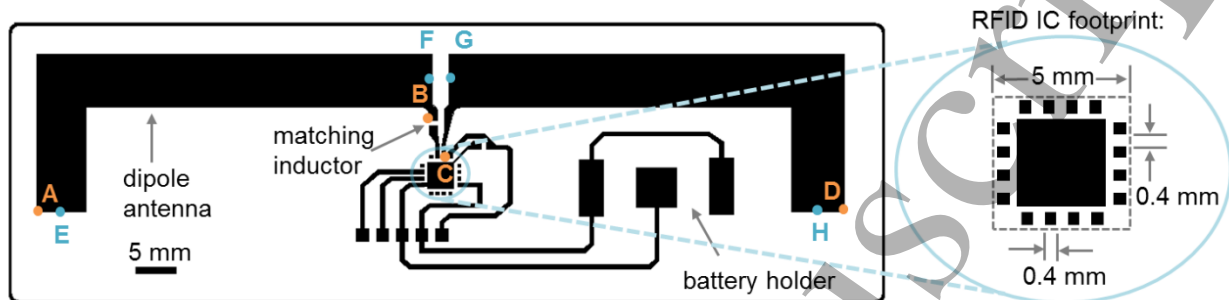


Figure 1. Tag design (110 mm × 35 mm) based on development kit for printing onto different substrates. A to B and C to D show the longest path over which resistance measurements are made for each antenna arm, while E to F and G to H show the centre paths over which resistance is measured.

2.2. Substrates

Table 1 lists the substrates that were utilized. These were selected based on their potential suitability to developing low-cost point-of-care diagnostic tests for health and environmental applications. The main categories for substrate selection are: 1) suitability to paper-based microfluidic implementations (category PM), 2) suitability to printed electronics (category PE), suitability to low cost, accessible, and practical uses, including both 3) direct application to flexible packaging (category FL) or 4) flexible sticker/adhesive formats that can be applied separately to a diagnostic device that may be manufactured on a different substrate (category FA), and 5) disposable, environmentally friendly biodegradable packaging (category BP). It should be noted that some substrates that have been specifically developed for printed electronics are also biodegradable. For truly environmentally friendly solutions to be realized, the disposability and biodegradability of all the inks and electronic components used would need to be considered. Costing of the different substrate categories varies with functionality and specialized properties. Costs are typically higher for specialized substrates that are suited to printed electronics or paper-based microfluidics, but vary substantially depending on the specific properties of the substrate.

2.3. Printing techniques

Manual screen printing of the tag designs was performed to illustrate printability. The screen was manufactured by Chemosol (Pty) Ltd. (Johannesburg, South Africa) using a synthetic mesh of 71 threads/cm (71/180-55 PW, SEFAR® PET 1500). Screen printing was carried out using a ZelPrint LT300 stencil printer (LPKF Laser and Electronics, Germany) with modifications made to enable screens to be manually mounted into the frame of the printer. A silver screen printable ink (AG-800, Applied Ink Solutions, USA) was used for screen printing with a rubber squeegee (70-75 Blue Apolan, Chemosol). Once printed, the devices were cured in an oven at 90 °C for 15 minutes.

2.4. Characterization of printed features

2.4.1. Print quality

Printed features were analysed using a brightfield microscope (Meiji Techno EMZ-8TR) with different magnifications (7× and 45×) to assess the consistency of the printing, the edge irregularities and resolution of fine detail, specifically for the IC pads. A laser scanning microscope (LSM 5 Pascal, Carl Zeiss, Germany) was utilized to assess the thickness and uniformity of the printed features on different substrates. Surface roughness measurements were conducted using LSM for both the substrate and the printed layer on the substrate to assess the effect of the substrate on the printed result. Three roughness measurements were conducted for each at a 200× magnification, with surface roughness calculated using the arithmetical mean roughness value (Ra). Six thickness measurements were also performed for each substrate using LSM. Measurements were performed across the antenna arms (200× magnification), with two devices analysed for each substrate. A theoretical wet print thickness of 28 µm is expected from the screen mesh used, and a corresponding reduction in thickness of down to 30% can be expected for the dried ink thickness, resulting in expected print thicknesses of approximately 8.4 µm.

Table 1. Overview of substrates grouped into categories according to their primary application.

	Label :	Substrate description:	Substrate characteristics:	Product:	Manufacturer:
Paper-based microfluidic substrates (PM)	PM1	Chromatography paper	Porous, suited for fluidic control	Whatman No. 1 CHR	GE Healthcare, UK
	PM2	Chromatography paper with wax melted through	Barriers for fluidic control and containment	Whatman No. 1 CHR with XER108R00749 - Xerox Black Solid Ink Stick	GE Healthcare, UK
Printed electronics substrates (PE)	PE1	Photo paper	Coated paper, suited to printed sensors, electronics, ink-jet printing	NB-RC-3GR120	Mitsubishi, Japan
	PE2	Polyethylene-naphthalate (PEN) film	Smooth, transparent film suited to flexible electronic applications	Teonix Q65HA (125 μ m)	DuPont Teijin Films, UK
	PE3	Polyethylene terephthalate (PET) film	Smooth, transparent film suited to flexible electronic applications	Melinex 506 (125 μ m)	DuPont Teijin Films, UK
	PE4	Ultra-smooth electronics paper	High-definition patterning of printed electronics	Powercoat HD 230	Arjowiggins Creative Papers, France
	PE5	Cellulosic electronics paper	High-throughput printed electronics	Powercoat XD 125	Arjowiggins Creative Papers, France
	PE6	Smart printed electronics paper	High dimensional stability of printed electronics, non-porous surface coating, hydrophilic primer layer	p_e: smart paper Type 1	Felix Schoeller Group, Germany
	PE7	Smart printed electronics paper	High dimensional stability of printed electronics, hydrophilic nano porous surface coating	p_e:smart paper Type 2	Felix Schoeller Group, Germany
	PE8	Polyester primered film	Heat stabilized polyester film, acrylic primered	Kemafoil MTSL W	Coveme, Italy
	PE9	Ceramic coated paper	Inorganic coated paper for electronics, absorbs solvents, low temperature sintering	Nano P60 paper	Printed Electronics Ltd, UK

	Label :	Substrate description:	Substrate characteristics:	Product:	Manufacturer:
Flexible, low-cost substrates (FL)	FL1	Standard printing paper	Readily available standard paper	Typek White Paper A4 80 GSM Premium	SAPPI, South Africa
	FL2	Cardboard packaging	Readily available packaging	Typek White Paper packaging box	SAPPI, South Africa
	FL3	Poly(methyl methacrylate) (PMMA)	Transparent, somewhat rigid, readily available plastic	AXSUHIC00125001250I Acroglas XTUHI SHT – 1 mm	Maizeys Plastics, South Africa
	FL4	Transparency/laser overhead projector film	Transparent and readily available film	17404081, Penguin Transparencies	Waltons, South Africa
Flexible, low-cost substrates with adhesive (FA)	FA1	Transparent adhesive vinyl	Transparent film with adhesive	Grafitack Promo P100 Transparent Film	Grafityp Selfadhesive Products N.V., Belgium
	FA2	Glossy adhesive vinyl	Glossy finish film with adhesive	Megarex D-MG Glossy Vinyl	X-Film, Germany
	FA3	Matt adhesive vinyl	Matt finish film with adhesive	Grafitack 1106 Black Film	Grafityp Selfadhesive Products N.V., Belgium
Biodegradable packaging substrates (BP)	BP1	Transparent, compostable, heat sealable film	Transparent, compostable, heat sealable film	NatureFlex NVR	Futamura Chemical Co. Ltd, Japan
	BP2	Transparent, compostable film	Transparent, compostable	NatureFlex NP	Futamura Chemical Co. Ltd, Japan

2.4.2. Electrical characterization

Resistance measurements and subsequent sheet resistance calculations were carried out for printed features on different substrates. Figure 1 indicates the points at which the resistance measurements were conducted on each printed antenna using an LCR meter (LCR-8110G, GW Instek, Taiwan) to perform four probe resistance measurements. Two devices were characterized for each substrate, resulting in four resistance measurements for each substrate. The sheet resistance (R_s) values were calculated from the resistance measurements (R) using

$$R_s = R \times w/l \quad (1)$$

where w is the width (7 mm), and l is the length (63 mm) of the printed antenna arm design across which the four probe resistance measurements are performed. The AG-800 silver ink used to print the devices has a sheet resistance of $< 0.015 \Omega/\text{sq}$ for a 25 μm layer.

2.5. Characterization of assembled tags

Assembly of the various components onto the printed RFID tags was performed using the brightfield microscope for visual alignment of the components onto the printed tracks. A two component silver epoxy conductive adhesive (186-3616 RS Pro Silver, RS Components, South Africa) was used to mount and secure the IC, 39 nH surface mount matching inductor (WE-MK multilayer ceramic, Würth Elektronik, Germany), and CR1220 3 V lithium manganese dioxide coin cell battery (CR1220, RS Pro, RS Components) with copper adhesive tape (3M Copper Foil Tape 1126, Digikey) to the printed RFID tag. The epoxy cured for 24 hours at room temperature. The inductor is connected on one of the antenna arms for impedance matching. Although the ideal value of this inductor varies according to the substrate used, and consequent input impedance, the value of 39 nH was implemented for all tags, as per the design implemented for the tag development kit. This allowed for relative comparisons to be made across all substrates, and eliminated the need for specialized antenna optimization software and characterization equipment which would be required to calculate the matching inductor values for each printed antenna.

The assembled RFID tags were characterized by performing read range measurements using the reader development kit (AS3993-QF_DK_R Fermi reader, AMS, Austria) which is recommended for use with the SL900A and includes a monopole antenna connected to a reader module. The focus of this study was to provide insight into the use of different flexible substrates for implementing read-out and wireless communication modules in real world settings. Read range measurements were thus performed as these are most important in terms of performance and practical implementation of the wireless communication, rather than focussing on optimization parameters for the antennas or transmission speeds. Maximum read ranges and received signal strength indicator (RSSI) values were recorded for each tag. RSSI is an indicator of signal strength from a tag to the RFID reader. Measurements were carried out for three tags for each type of substrate, both in passive (no battery) and active (battery-assisted) modes. Figure 2 shows the measurement set-up with a sliding mechanism for adjusting the height of the mounted reader antenna, as well positioning for testing different tag orientations.

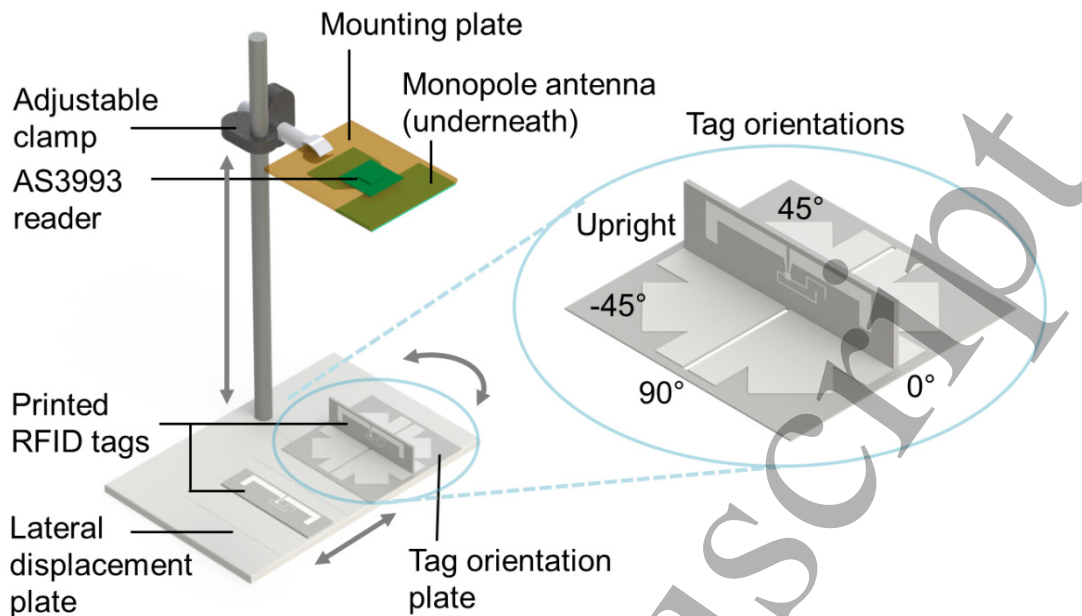


Figure 2. Measurement set-up for testing the printed RFID tags. The reader antenna and reader are connected via USB to a personal computer and measurements are captured through a user interface.

3. Results

Figure 3 shows selected examples of printed tags onto different substrates, along with the complete assembled tags which were tested for read-out and wireless communication functionality.

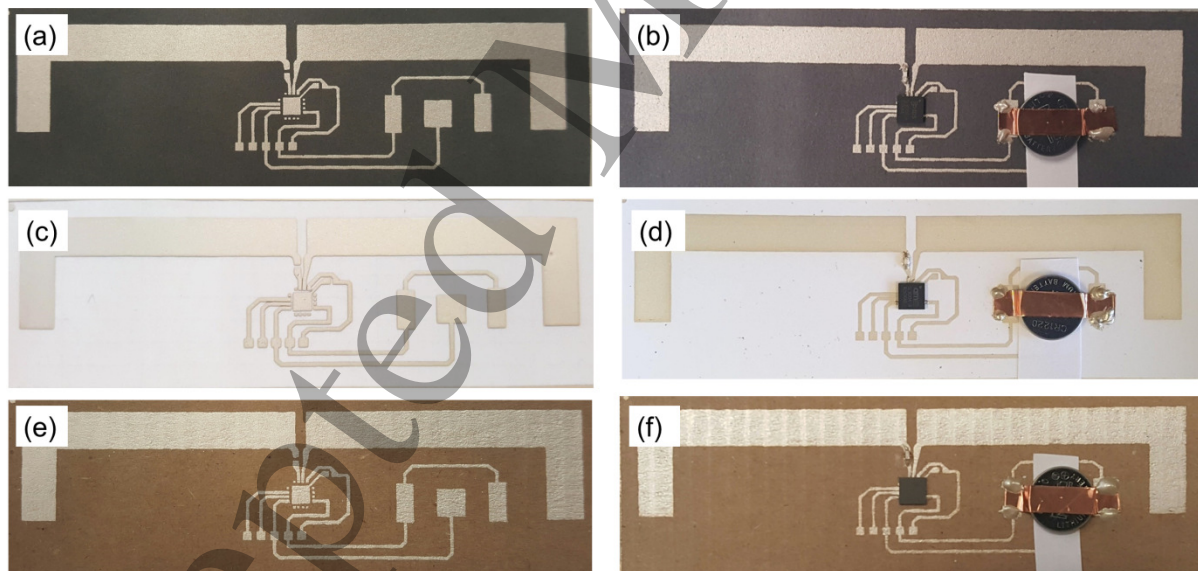


Figure 3. Examples of printed tags onto different substrates (left) and complete assembled tags for read out and wireless communication testing (right). Substrate examples shown are PM2 (a,b) PE9 (c,d) and FL2 (e,f).

3.1. Printed features

Brightfield microscopy was used for visual assessment of print quality. LSM scans enabled surface roughness and thickness measurements. Substrate and printed layer roughness and thickness were verified using surface profilometry (Form Talysurf PGI 820, Taylor Hobson, UK) for selected substrates and produced comparable results.

LSM scans at 200× magnification produced surface profiles at the boundary between the substrate and the printed ink layer, to enable print thickness measurements to be made. Thickness measurements varied across substrates and different devices as a result of the manual screen printing process. The average measured thickness across all substrates and devices (60 measurements in total) gave an average thickness of 7.82 μm (SD 3.27 μm). The average thicknesses of the printed ink for all substrates ranged between 4 μm and 16 μm , with large fluctuations from 1.5 μm to 23 μm noted in the PM substrates.

Figure 4 shows the roughness measurements obtained using LSM, along with sample brightfield microscopy and LSM images. Paper-based microfluidic substrates (PM) as well as printing paper and cardboard packaging (FL1 and FL2) produced the highest substrate roughness measurements, with the roughness of the print lower than the substrate as a result of the fibrous substrate being coated by the ink. Printed electronics substrate PE5 is a cellulose-based substrate with a roughness specification of 1.5 μm , which is similar to the measured result and is rougher than many of the other specialized PE substrates. The printed layer on this and slightly rougher substrate FA3 is smoother than the substrate, with the ink coating the fibres and rough substrate surfaces. The majority of PE substrates and other smooth substrates in the FL and FA categories have very smooth substrates with roughness values well below 1 μm , and corresponding print roughness values substantially higher than that of the substrate. Substrate PE4 has a large printed layer roughness arising from bubbles forming in the print. This is likely a result of the solvent phase in the ink that dissolves a binder component in the coating of the paper. This does not occur with aqueous ink and does not degrade the conductivity.

Sheet resistance measurements are also shown in Figure 4, with standard deviations across four resistance measurements are indicated for each substrate. Using the average thickness value of 7.82 μm obtained from LSM measurements across all tags, a theoretical calculated sheet resistance of 0.048 Ω/sq was obtained. The average experimentally calculated sheet resistance for all substrates is 0.07 Ω/sq (SD = 0.057 Ω/sq). Many of the individual sheet resistance values fall within or close to this range, with large outliers being the BP substrates.

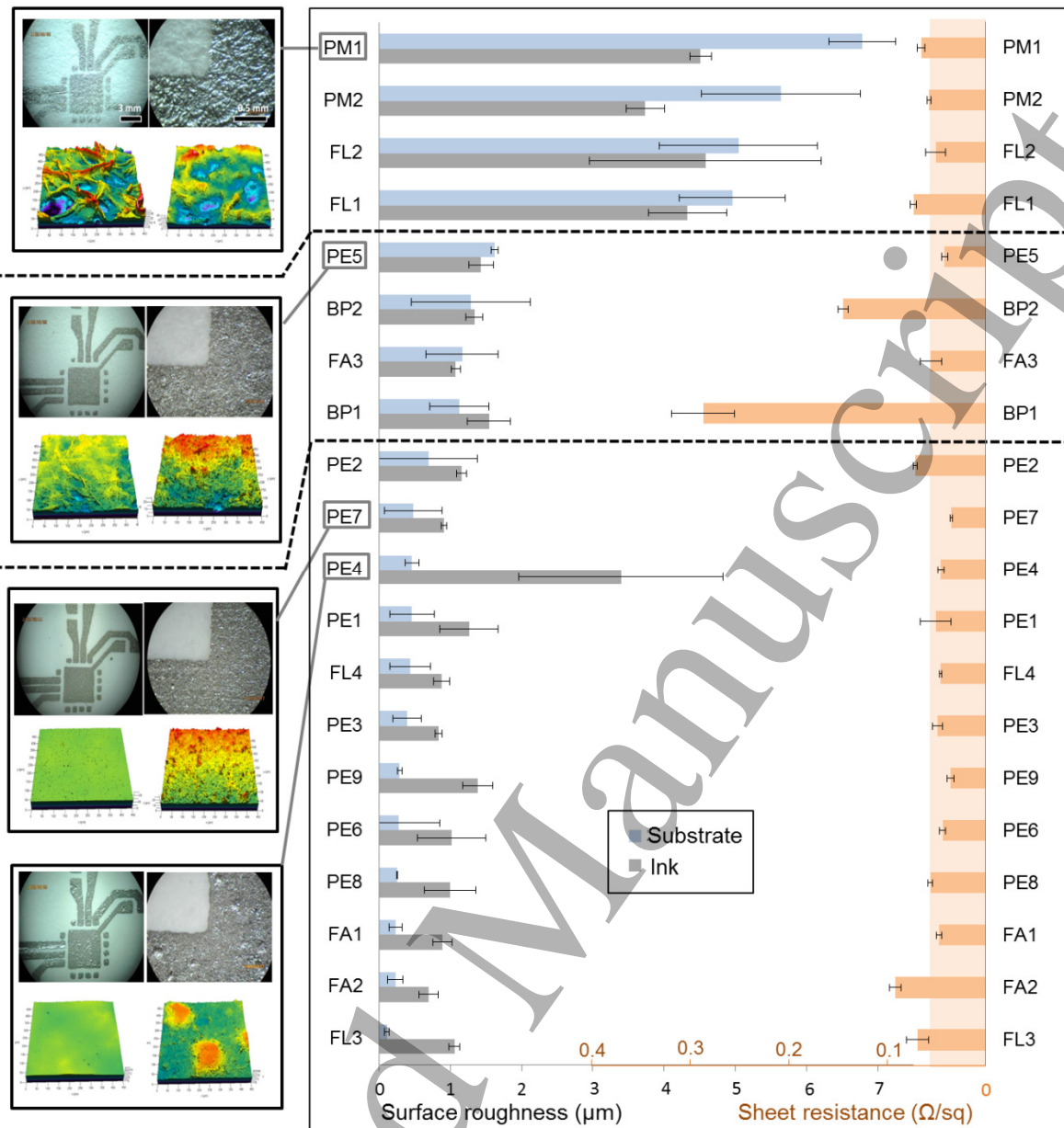


Figure 4. Substrate and print roughness measurements for various substrates along with corresponding sheet resistance values.

3.2. Assembled tags

Figure 5 shows the read range measurements obtained using the set-up shown in Figure 2. The read range is defined as the maximum distance at which the tag can successfully be detected by the reader. The maximum distance for successful read-out of the temperature sensor value (on-board the SL900A IC) from the tag was also recorded. Three devices were tested for each type of substrate – both with and without a battery. For each tag scanned, the corresponding RSSI was recorded. The reader antenna used was the monopole from the development kit with a gain of 2.2 dBi. The power transmitted by the reader is 22 dBm, giving an effective isotropic radiated power (EIRP) of 24.2 dBm assuming no cable losses. Reader settings were selected with Korea (917 – 920 MHz) as the region, as this covers the standard South African frequency range for RFID (915 – 919 MHz). The reader sensitivity was left at -68 dBm, the default setting in the GUI, which sets the AS3993 reader IC sensitivity to -68 dBm. Assuming a distance of 0.5 m between the RFID reader and tag, an example of

1
2
3 the RFID link budget, which takes into account the various gains and losses in the system, can be
4 estimated. Path loss is a function of the wavelength and the distance between the tag and the reader.
5 The forward link or power incident on the tag is determined as: reader transmit power (EIRP) + path
6 loss = 24.2 dBm - 25.6 dB = -1.4 dBm. The wake up power of the SL900A IC in passive mode is 0.2
7 mW (sensitivity = -7 dBm), thus the forward link has enough power to power on the tag IC. The
8 reverse link or the power received by the reader from the backscattered tag signal is determined as:
9 power incident on tag + modulation loss + path loss = -1.4 dBm - 10 dB - 25.7 dB = -37 dBm
10 (assuming a typical modulation loss of -10 dB). Thus the reader can detect the incoming tag signal
11 of -37 dBm, as the reader is more sensitive (-68 dBm). However, this does not take in to account any
12 additional losses that may be present in the system or that may be introduced by the manually
13 assembled tags on different substrates.
14
15

16
17 Read ranges of between 75 mm and 300 mm were measured for tags in passive mode (average of
18 212.1 mm for tag detection (SD 78.9 mm) and 177.5 mm for temperature readout (SD 66.8 mm)),
19 and between 150 mm and 400 mm for active mode (average of 352.4 mm for tag detection (SD 137.4
20 mm) and 300.8 mm for temperature readout (SD 96.7 mm)), excluding the benchmark development
21 kit device (CB1) which had slightly higher read ranges of more than 900 mm in active mode. Longer
22 read ranges are achieved in active mode as expected, and variations in the read ranges for the same
23 substrate can be noted as a result of manual fabrication and assembly of the individual tags. The
24 average RSSI values recorded for the various tags range from -44 dBm to -40 dBm for passive mode
25 and -54 dBm to -47 dBm for tags in active mode. Large variations in RSSI values can be noted for
26 PE4, potentially as a result of the print quality affecting the tag measurements.
27
28

29
30 Read range results were also performed by commercial RFID company Synertech (Pty) Ltd
31 (Johannesburg, South Africa) with a commonly used commercial RFID reader (Impinj Speedway
32 Revolution R420, Impinj, USA), circularly polarized reader antenna (SF-1101, Flexiray, Czech
33 Republic) with a gain of 0 dBi, and with region setting South Africa. The reader settings were
34 adjusted in the software and included a reader transmit power of 26 dBm and a receive sensitivity of -
35 70 dBm. The measurements showed that all printed tags were functional with read ranges between
36 170 mm to 510 mm obtained for tags in passive mode, and between 313 and 863 mm in active mode.
37 RSSI values obtained ranged from -46 dBm to -39 dBm for passive tags and -63 dBm to -46 dBm for
38 active tags. Longer read ranges were obtained compared to the development kit reader measurements
39 as a result of the difference in reader antenna properties and settings.
40
41

42
43 To assess practical tag functionality further, individual tags for 9 selected substrates (Table 2) were
44 analysed to determine the effect of distance between the tag and the reader on the RSSI values (Figure
45 6). RSSI values over distance were also tested with a load connected to the SL900A for each tag to
46 simulate a practical application towards an integrated point-of-care diagnostic solution. This entailed
47 components attached to both EXT1 and EXT2 pins of the IC mounted to the tag, as resistive and
48 optical sensor inputs, namely a 100 k Ω resistor and an optical sensor (VTB8440B photodiode,
49 PerkinElmer Optoelectronics, USA), respectively, as well as a 575 nm green LED (TLLG4400,
50 Vishay, USA) connected between the battery supply for potential user feedback or displaying of
51 results.
52
53

54
55 To further understand the practical functionality of the printed tags, read ranges for different tag
56 orientations were recorded. The default 0° orientation provides optimal read range results, but in a
57 practical situation the tag orientation could vary. The set-up used for the orientation tests is shown in
58 Figure 2, with results presented in Figure 7 and summarized in Figure 8 to illustrate the overall effect
59 of tag orientation on the readability of the tags.
60

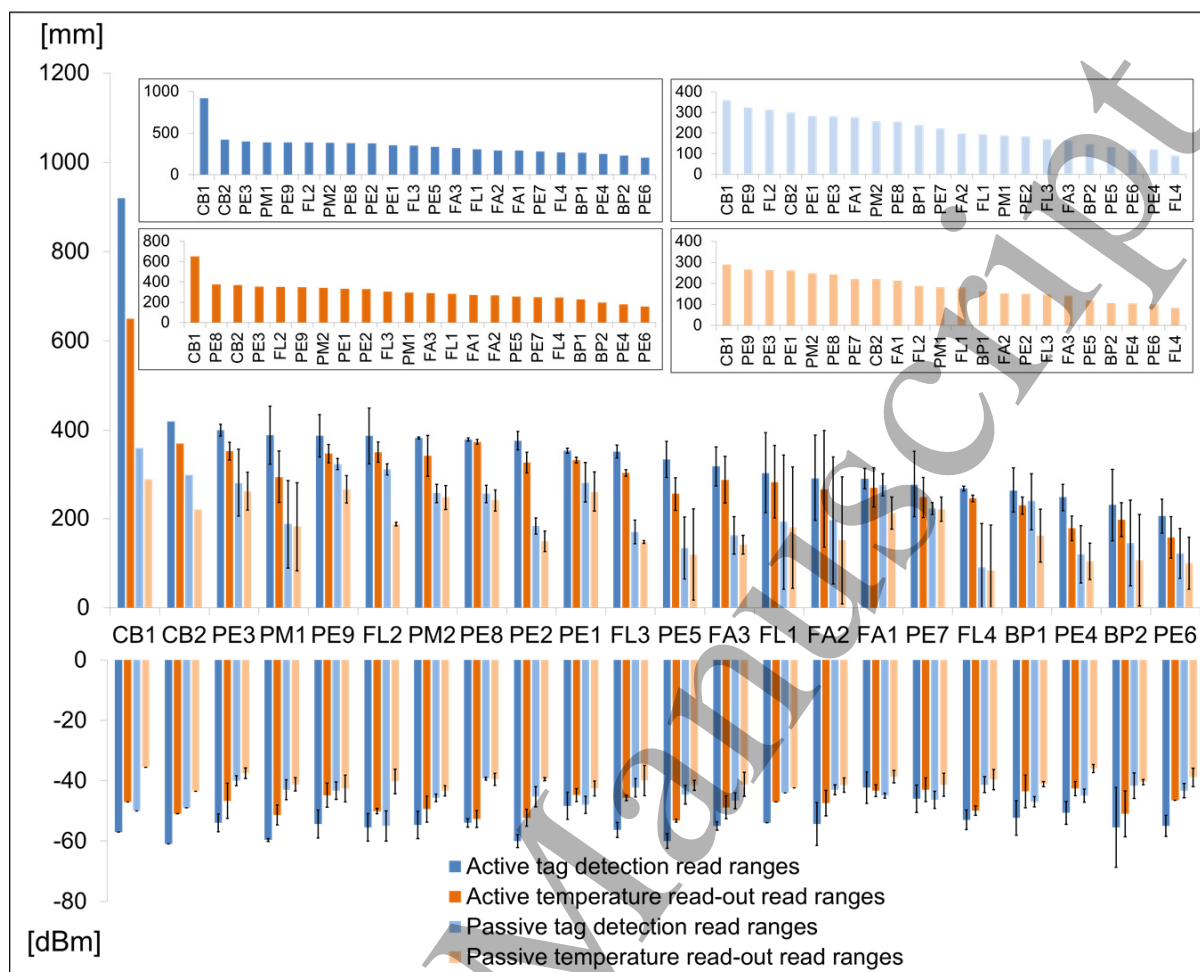


Figure 5. Maximum read ranges and RSSI values recorded for 3 tags per substrate type. Active and passive modes were investigated, both for tag detection (blue) and sensor readout (orange). Insets show ordering of read ranges from highest to lowest across the substrates for each of the tag readout modes.

Table 2. Selected tag substrates for performing further practical functionality testing.

Substrate	Description
CB1	Development kit PCB: benchmark device for comparing to printed devices
CB2	Milled PCB: benchmark manually assembled device for comparing to printed devices
PE3	Printed electronics substrate: performs well with large read ranges achieved
PM2	Chromatography paper with wax: typically used for paper-based microfluidics
PE1	Photo paper: standard substrate for printed electronics, particularly inkjet printing
FA2	Adhesive substrate: large variations in read range performance
FL4	Transparency: low-cost substrate, poor performance without battery
PE6	Printed electronics substrate: lower read ranges recorded

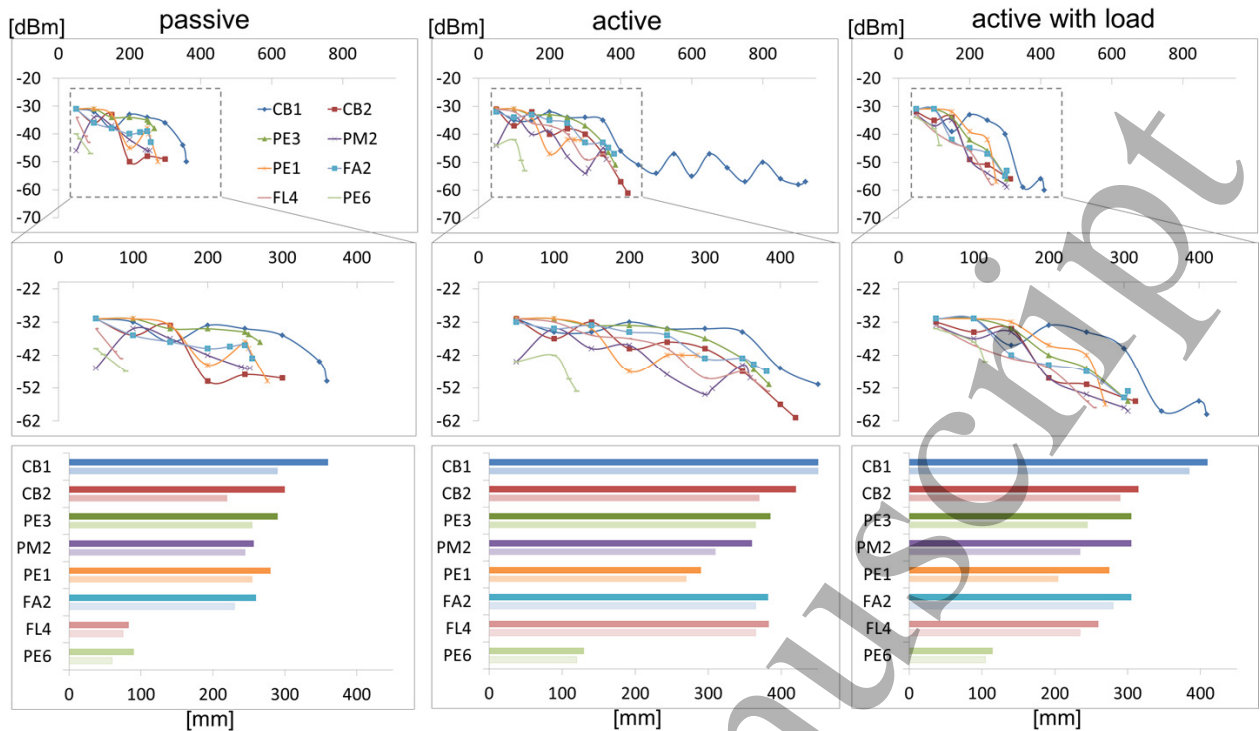


Figure 6. RSSI over distance with maximum read ranges for individual tags of selected substrates to illustrate practical functionality in passive and active modes, as well as with a load connected.

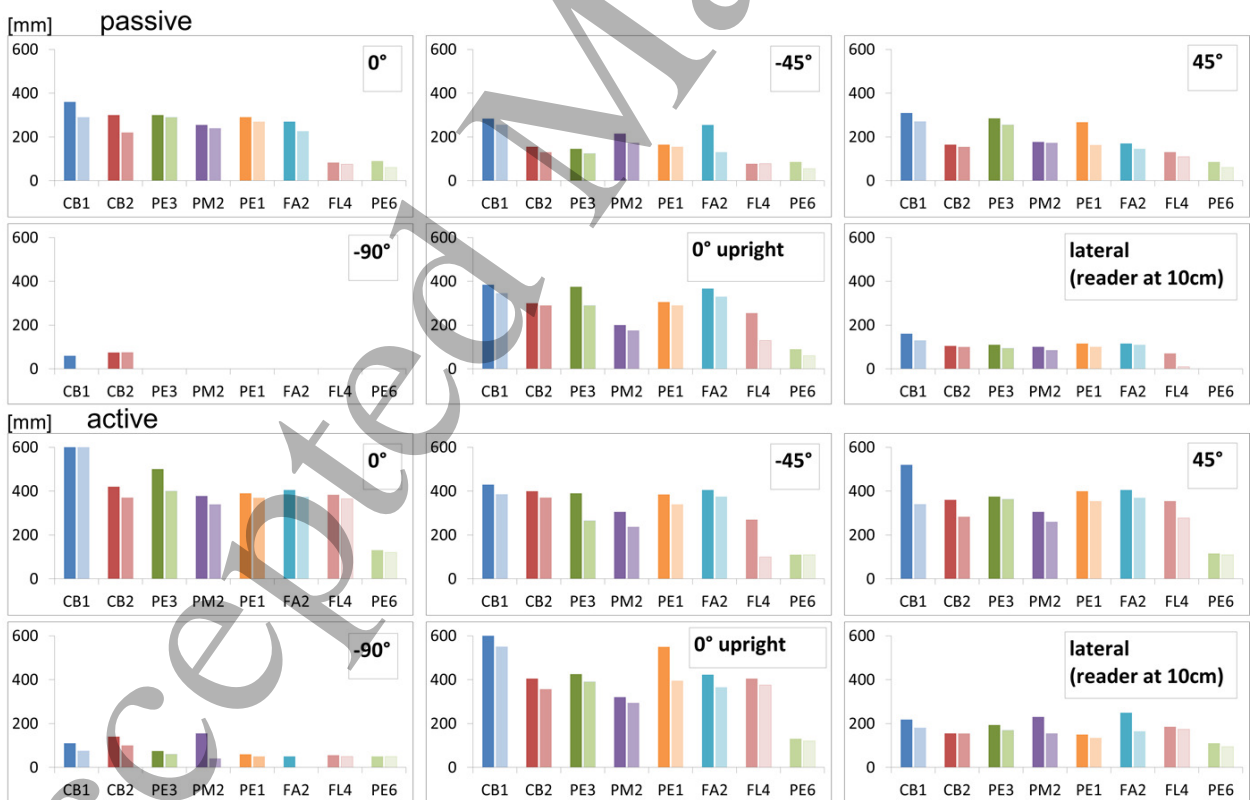


Figure 7. Maximum read range results for different tag orientation for 8 selected substrates in both passive and active mode. Maximum read ranges for successful detection are shown in darker colours and corresponding maximum read ranges for successful temperature readout in lighter colours.

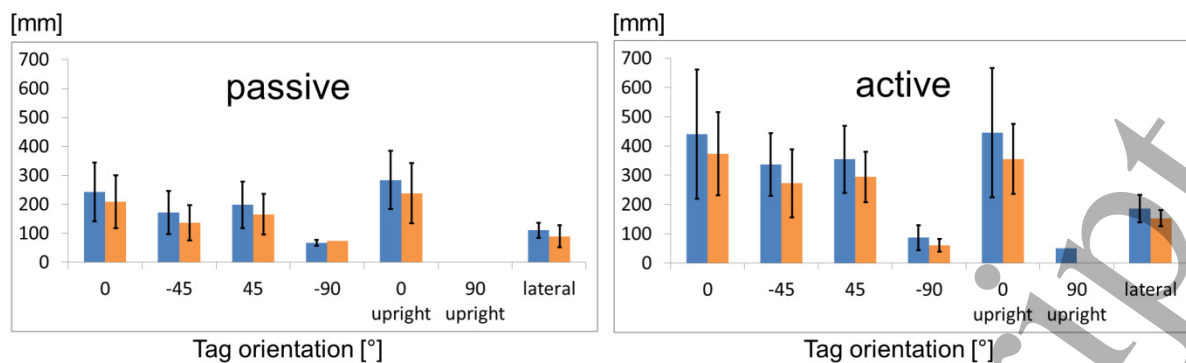


Figure 8. Summary of tag orientation results across 8 different substrates. Average maximum read ranges for successful detection (blue) and temperature read-out (orange) are shown to illustrate trends for varying orientations in both passive and active mode.

4. Discussion

This work illustrates the feasibility of implementing printed UHF RFID tags with sensing capabilities onto different substrates, with focus on low-cost point-of-care diagnostic device development. A manual screen printing set-up and assembly process enabled low-cost, rapid prototyping of devices which could be assessed in terms of practical functionality.

Surface roughness measurements for substrates and printed ink layers (Figure 4) showed two main trends: 1) fibrous substrates high in roughness had a smoother print layer, with the ink coating the fibres and filling the irregular spaces, and 2) smoother substrates resulted in print layers with increased roughness with values in the range of 1 – 1.5 μ m, independent of the substrate roughness. Outliers in print quality such as PE4 highlight the need to consider the ink composition and its compatibility with the substrate being used to avoid print irregularities. Complete sets of brightfield microscopy images, LSM images and roughness measurements for each substrate can be found in Appendix 1: Supplementary Information.

Printed thickness variations result from the manual screen printing process and variations in the substrate structures. Resulting sheet resistance values were comparable to the value provided for the silver ink on most of the substrates, but with large resistances noted for the BP substrates (Figure 5), where the extreme flexibility and warping of the substrates could affect the print uniformity and thus conductivity. However, paper-based substrates can be incinerated and thus biodegradability need not be a primary concern, and the substrate to be utilized should be chosen according to the desired properties for the application, be it fluidic, electronic or other. PE substrates generally have the lowest sheet resistance values as expected as these are designed specifically for printed electronics. Print quality does not have a direct effect on the resistances of the printed tags, but for fibrous substrates such as PM1, PM2 and FL2, this could result in increased ink coated surface areas, which contribute to improving the read ranges of these tags (Figure 5).

Suitability of the assembled tags to practical applications was assessed through read range measurements, which showed a high degree of functionality (Figure 5). All 60 printed tags tested were operational, with minimum read ranges of 75 mm achieved in passive mode. This is adequate for the purposes of the intended point-of-care diagnostic applications for contactless and contamination-free communication of results from the test device. Maximum read ranges for the development kit in this work were around 900 mm in active mode and 360 mm in passive mode, and used as a comparative baseline. Other research that utilized the SL900A and carried out optimization of the

1
2
3 antenna design and impedance matching achieved read ranges of between 800 mm and 1100 mm in
4 passive mode [18-21]. These are generally implemented on optimal substrates using high precision
5 printing techniques and each with different antenna and reader settings. The development kit tag and
6 reader manufacturer reports a read range of up to 2 m achievable in active mode, but this can be
7 affected by a number of parameters including antenna gain, antenna polarization, output power, reader
8 sensitivity, transponder (SL900A IC) antenna type, which are not specified for this result. Variations
9 in read range and RSSI values in this work can also be attributed to the manual printing and assembly
10 procedures, as well as environmental factors as the tags were tested in a standard laboratory, where
11 reflections in the RF signal can occur. Impedance mismatch and poor antenna gain can be caused by
12 printing, and could be improved by printing thicker, more uniform layers [21]. The printing technique
13 used can also affect the performance of the RFID tag, but can still produce reliable tags [22], which is
14 the ultimate goal of this work. Practical functionality of the tags is the objective rather than
15 optimization of the antenna properties, using an existing tag design and testing the repeatability and
16 reliability of this for practical applications. The results show that if the working distance is chosen to
17 be below 50 mm, functional tags can be realized on any of the substrates utilized in this study. Thus
18 the substrate can be selected according to other performance parameters and the application required.
19
20
21
22

23 Individual tags for selected substrates were tested to investigate the variation in signal strength
24 received as a function of distance, and showed a decrease in RSSI as the distance increased (Figure 6).
25 Typical RSSI ranges utilized by Synertech includes a -80 dBm cut-off, where a tag is typically no
26 longer classified as readable, and a maximum received signal strength of a tag of -20 dBm as a
27 standard measure of performance. RSSI values between -35 dBm and -30 dBm are considered to be
28 indicative of high performance tags, but are often difficult to achieve in real world conditions. The
29 RSSI values recorded for the various tags in this study range from -60 dBm to -35 dBm, with all
30 values still well within the acceptable performance range. The sensitivity of the reader will affect the
31 RSSI values recorded, as an increase in sensitivity will allow for weaker tags (lower RSSI values) to
32 be recorded.
33
34
35

36 Trends in the RSSI values and resulting maximum read ranges for the selected substrates are
37 comparable for passive, active, and active with load scenarios. Read ranges are lower with a load
38 connected than in active mode with a battery, but tag performance is adequate, with read ranges in
39 excess of 100 mm achievable with a load comprising an LED and two sensors inputs. This showcases
40 sufficient functionality for practical applications. Future implementations could include all-printed
41 sensors, displays and power-sources combined with the tag for a fully integrated solution. The power
42 settings of the reader will affect the measurements, where an increase in 3 dB doubles the power, and
43 thus increases the read range. This will be an important consideration for practical implementations in
44 clinics, where power could be restricted and a trade-off should be made between acceptable read
45 ranges and resource constraints, along with cost.
46
47
48

49 Tag orientation, angle and placement all play a role in the read ranges achievable, as seen from
50 Figures 7 and 8. An orientation of 0° is optimal for all tags, while at -90° upright, only the
51 development kit tag (CB1) can be detected in active mode. An orientation of -90° results in the
52 poorest tag performance with compromised read ranges. Lateral displacement of tags was also found
53 to give poor performance, particularly for antenna reader heights exceeding 200 mm, where most tags
54 could no longer be detected for any displacement distance tested. In practical settings, tag orientation
55 is an important consideration, but could be implemented in such a way that the scanning set-up
56 adheres to a range of tag orientations that would produce a working result, for example by using a tag
57 holder or mounting mechanism.
58
59
60

1
2
3
4
5 This work confirms that for acceptable read ranges of approximately 50 mm, reliable RFID readout
6 can be achieved for tags printed onto different substrates suited to point-of-care diagnostic
7 applications. Automated screen printing could be used in future development once successful
8 prototypes have been realized, and can be scaled up for mass production using roll-to-roll techniques
9 and lowering the cost of devices.
10

11 **5. Conclusions**

12
13
14 This work demonstrates wireless connectivity using manually screen printed and assembled low-cost
15 RFID tags that were effectively implemented on a large variety of substrates – including low-cost,
16 readily accessible substrates with direct application to or integration with paper-based diagnostic
17 solutions. Future work could be extended to more detailed characterization of the RFID antennas,
18 where characterization and modelling could reveal insights into the different substrates and optimal
19 uses thereof. However, the focus of this work was to determine the feasibility of using different
20 substrates suited to low-cost point-of-care diagnostics for wireless connectivity modules. The work
21 shows that practical, functional RFID tags with built-in sensing capabilities can be implemented
22 successfully towards integrated, automated and connected low-cost point-of-care diagnostic solutions.
23 Thus future research can be built on the assumption that a reliable link to the outside world exists and
24 will focus on the electrical readout of the diagnostic result on paper. The solutions are poised to meet
25 the ASSURED criteria and to solve many of the challenges faced in diagnostic testing carried out at
26 rural and resource-limited healthcare facilities.
27
28
29

30 **Acknowledgements**

31
32 The authors gratefully acknowledge the Council for Scientific and Industrial Research (CSIR),
33 Pretoria, South Africa, as well as Karlsruhe Institute of Technology (KIT), Germany, for financial
34 support. The authors would like to thank Synertech (Pty) Ltd, South Africa for their expertise in RFID
35 and assistance with antenna read range measurements. The authors also thank Louis Fourie at the
36 CSIR for conducting laser scanning microscopy experiments, and Oelof Kruger at the National
37 Metrology Institute of South Africa (NMISA), South Africa, for conducting profilometry
38 measurements.
39
40
41

42 **References**

- 43
44 [1] Mabey, D., Peeling, R. W., Ustianowski, A. and Perkins, M. D. (2004). Diagnostics for the
45 developing world. *Nature Reviews Microbiology*, 2(3), 231–240.
46
47 [2] Engel, N., Davids, M., Blankvoort, N., Pai, N. P., Dheda, K. and Pai, M. (2015). Compounding
48 diagnostic delays: a qualitative study of point-of-care testing in South Africa, *Tropical Medicine and*
49 *International Health*, 20(4), 493–500.
50
51 [3] Meyer, W. D. (2013). Connectivity in point of care testing. *PathCare Pathology Forum - Point of*
52 *Care*, 1st Edition, 4(2), 24–25.
53
54 [4] Yetisen, A. K., Akram, M. S. and Lowe, C. R. (2013). Paper-based microfluidic point-of-care
55 diagnostic devices. *Lab on a Chip*, 13(12), 2210–2251.
56
57
58
59
60

- [5] Yamada, K., Shibata, H., Suzuki, K. and Citterio, D. (2017). Toward practical application of paper-based microfluidics for medical diagnostics: state-of-the-art and challenges. *Lab on a Chip*, 17(7), 1206–1249.
- [6] Chang, J. S., Facchetti, A. F. and Reuss, R. (2017). A circuits and systems perspective of organic / printed electronics : review, challenges, and contemporary and emerging design approaches, *IEEE Journal on Emerging and Selected Topics in Circuits and Systems*, 7(1), 7–26.
- [7] Beni, V., Nilsson, D., Arven, P., Norberg, P., Gustafsson, G. and Turner, A. P. F. (2015). Printed electrochemical instruments for biosensors. *ECS Journal of Solid State Science and Technology*, 4(10), S3001–S3005.
- [8] Ahmadraji, T., *et al.* (2017). Biomedical diagnostics enabled by integrated organic and printed electronics. *Analytical Chemistry*, 89(14), 7447–7454.
- [9] Salmerón, J. F., Molina-Lopez, F., Briand, D., Ruan, J. J., Rivadeneyra, A., Carvajal, M. A., Capitán-Vallvey, L. F., Derooij, N. F. and Palma, A. J. (2014). Properties and printability of inkjet and screen-printed silver patterns for RFID antennas. *Journal of Electronic Materials*, 43(2), 604–617.
- [10] He, H., Sydänheimo, L., Virkki, J. and Ukkonen, L. (2016). Experimental study on inkjet-printed passive UHF RFID tags on versatile paper-based substrates, *International Journal of Antennas and Propagation*, 2016, ID 9265159, 1–8.
- [11] Kavčič, U., Pivar, M., Dokić, M., Svetec, D. G., Pavlovič, L. and Muck, T. (2014). UHF RFID tags with printed antennas on recycled papers and cardboards. *Materials and Technology*, 48(2), 261–267.
- [12] Kavčič, U., Maček, M. and Muck, T. (2015). Ultra-high frequency radio frequency identification tag antennas printed directly onto cardboard used for the manufacture of pharmaceutical packaging. *Journal of Imaging Science and Technology*, 59(5), 50504-1–50504-8.
- [13] Smith, S., Land, K., Korvink, J. G. and Mager, D. (2017). Connected , low-cost point-of-care diagnostics for rural South African clinics. *MicroTAS 2017: 21st International Conference on Miniaturized Systems for Chemistry and Life Sciences*, 657-658.
- [14] Smith, S., Bezuidenhout, P. H., Land, K., Korvink, J. G. and Mager, D. (2017). Development of paper-based wireless communication modules for point-of-care diagnostic applications. *Proceedings of SPIE*, 10036, 100360J.
- [15] Tomaszewski, G., Jankowski-Mihulowicz, P., Weglarski, M. and Lichoń, W. (2016). Inkjet-printed flexible RFID antenna for UHF RFID transponders. *Materials Science-Poland*, 34(4), 760–769.
- [16] Salmeron, J. F., Molina-Lopez, F., Rivadeneyra, A., Quintero, A. V., Capitán-Vallvey, L. F., De Rooij, N. F., Ozáez, J. B., Briand, D. and Palma, A. J. (2014). Design and development of sensing RFID tags on flexible foil compatible with EPC Gen 2. *IEEE Sensors Journal*, 14(12), 4361–4371.
- [17] Fernández-Salmerón, J., Rivadeneyra, A., Martínez-Martí, F., Capitán-Vallvey, L. F., Palma, A. J. and Carvajal, M. A. (2015). Passive UHF RFID tag with multiple sensing capabilities. *Sensors*, 15(10), 26769–26782.

1
2
3 [18] Escobedo-Araque, P., Martínez-Olmos, A., Carvajal, M. Á. and Palma, A. J. (2015). Passive
4 UHF RFID tag for spectral fingerprint measurement, *2015 IEEE 15th Mediterranean Microwave*
5 *Symposium (MMS)*, 1–4.
6

7 [19] Escobedo, P., Carvajal, M. A., Capitán-Vallvey, L. F., Fernández-Salmerón, J., Martínez-Olmos,
8 A. and Palma, A. J. (2016). Passive UHF RFID tag for multispectral assessment, *Sensors*, 16(7),
9 1085, 1–13.
10

11 [20] Salmerón, J. F., Rivadeneyra, A., Agudo-Acemel, M., Capitán-Vallvey, L. F., Banqueri, J.,
12 Carvajal, M. A. and Palma, A. J. (2014). Printed single-chip UHF passive radio frequency
13 identification tags with sensing capability. *Sensors and Actuators, A: Physical*, 220, 281–289.
14

15 [21] Falco, A., Salmerón, J. F., Loghin, F. C., Lugli, P., and Rivadeneyra, A. (2017). Fully printed
16 flexible single-chip rfid tag with light detection capabilities. *Sensors*, 17, 534,1–12.
17

18 [22] Björninen, T., Merilampi, S., Ukkonen, L., Sydänheimo, L. and Ruuskanen, P. (2009). The effect
19 of fabrication method on passive UHF RFID tag performance. *International Journal of Antennas and*
20 *Propagation*, 2009, ID 920947, 1–8.
21
22
23
24
25
26
27
28
29
30
31
32
33
34
35
36
37
38
39
40
41
42
43
44
45
46
47
48
49
50
51
52
53
54
55
56
57
58
59
60